Supplemental Information

Epstein-Barr Viral Productive Amplification Reprograms Nuclear Architecture, DNA Replication and Histone Deposition

Ya-Fang Chiu, Arthur U. Sugden, and Bill Sugden

SUPPLEMENTAL INVENTORY

Supplemental items Main items

Figure S1**,** related to Figure 1

Figure S2**,** related to Figure 3

Figure S3**,** related to Figure 4

Figure S4**,** related to Figure 5

Figure S5**,** related to Figure 6

Table S1**,** related to Experimental Procedures

Supplemental Figure Legends

Figure S1, related to Figure 1. Shown is the digestion pattern of Visible EBV's genome, detection of the fluorescent signals in cells carrying latently established Visible Amplicon or Visible EBV, and the fluorescent signals in B cells transformed by Visible EBV. (A) The 2089 and Visible EBV recombinant plasmids isolated from *E. coli* were digested with *Bam*HI and separated on an agarose gel. (B-C) The Visible Amplicon (B) and Visible EBV (C) in iD98/HR1 and i293 cells, respectively, were detected under a fluorescence microscope after removal of IPTG from the medium. Images acquired from a single focal plane are shown. (D) One primary B cell was infected with Visible EBV and the proliferating B cell was characterized after one month by detecting LacI-tdTomato fluorescent signals after removal of IPTG from the medium with a fluorescence microscope. The compressed image from multiple z-planes is shown. Z-stacks with 84 planes separated by 0.35 μm were acquired for each experiment. (E-H) mRNA from iD98/HR1 cells was isolated 0, 12, 24, 36, 48 and 60 hr post-induction with tamoxifen and levels of *BRLF1* (E), *BALF5* (F), *BMRF1* (G) and *BcLF1* (H) were determined by qPCR. The expression levels were normalized to that of *GAPDH*, and then compared to expression levels in the absence of tamoxifen, which was arbitrarily set to 1. Data represent the average of two independent experiments ± s.d.

Figure S2, related to Figure 3. Visualization of EBV derivatives in the productive cycle by live-cell imaging. (A-C) i293(visible EBV) cells were treated with

tamoxifen and tracked every hour over a 60-hour period by time-lapse microscopy. The sum of intensities of the fluorescent signals in each nucleus for amplified Visible EBV was determined with CAPS over time and their increases plotted. The arrows indicate two daughter cells derived from a parent after treatment with tamoxifen; each daughter was tracked and shown (B and C). (D) A numerical summary of an experiment with both i293 cells without Visible EBV transduced to express LacI-tdTomato fusions and i293(Visible EBV) cells carried with or without IPTG and followed after treatment with tamoxifen is shown. Fluorescent signals of LacI-tdTomato were detected only in i293(Visible EBV) cells after removing IPTG in the both latent and productive phases of EBV life cycle showing the dependence of the signals on the presence of Visible EBV DNA derivatives.

Figure S3, related to Figure 4. Distribution of PCNA and formation of EBV Amplification factories. (A-B) Shown is eGFP-PCNA in iD98/HR1(Visible Amplicon) cells treated with tamoxifen. The cell in (A) did not pass through mitosis prior to amplification; that in (B) did. In both (A) and (B) PCNA is redistributed as viral DNA is amplified. The cells were tracked every two hours over 60 hours by time-lapse microscopy. The arrows indicate the two daughter cells which divided after treatment with tamoxifen and were tracked. (C) The altered distribution of PCNA in EBV's amplification factories was most apparent following fixation and imaging with a Zeiss Apotome microscope.

Figure S4, related to Figure 5. The distribution of EBV derivatives and eGFP-histone fusions during the productive cycle were tracked by live-cell imaging or analyzed as fixed samples with an Apotome microscope. (A-C) The iD98/HR1(Visible Amplicon) (A) and i293(Visible EBV) (B and C) cells were transduced to express eGFP-histone H2B fusions followed by treatment with tamoxifen and tracked every two hours over 60 hours by time-lapse microscopy. The sum of intensities of eGFP fluorescent signals (green circles) for eGFP-H2B and Red fluorescent signals (red circles) for amplified Visible Amplicon or Visible EBV in identical volumes was determined with CAPS, plotted, and show that histone signals do not increase as EBV DNA signals grow. (D-H) The iD98/HR1(visible Amplicon) (E, F) and i293(visible EBV) cells (D, G, H) were transduced to express eGFP-histone H2B (D), H3.1 (E, G) and H3.3 (F, H) fusions followed by treatment without (D, a-c; E, a-c; F, a-c; G, a-c; H, a-c) or with tamoxifen (D, d-f; E, d-i; F, d-i; G, d-f; H, d-f) for 24 hr (E, d-f; F, d-f), 36 hr (E, g-i; F, g-i), or 48 hr (D, d-f; G, d-f; H, d-f) and fixation with paraformaldehyde after removal of IPTG from the medium. The distribution of Visible Amplicon, Visible EBV, eGFP-H2B, eGFP-H3.1 and eGFP-H3.3 fusions was detected with a Zeiss Apotome microscope.

Figure S5, related to Figure 6. The distribution and deposition of histones. (A) B95.8 cells were transfected to express eGFP-H2B followed by treatment with 12-*O*-tetradecanoyl-phorbol-13-acetate (TPA) and sodium butyrate for 48 hr. Both fixed and live cells display structures in the nuclei characteristic of EBV's

amplification factories. The arrows indicate that one cell was imaged in both bright field and with fluorescence to show that the imaged cells were alive. (B) i293 (without Visible EBV) (left) or iD98/HR1 cells harboring a variant of EBV (Glaser and Rapp, 1972), but not Visible Amplicon (right) were transduced to express eGFP-H2B and treated with tamoxifen for 34 hr. The distributions of eGFP-H2B were detected in fixed cells and by live-cell imaging. The iD98/HR1 cells treated with tamoxifen, but not ethanol (served as a negative control), have nuclear structures with the margined eGFP-H2B. (C-D) The introduction of five otherwise inhibited histone chaperones did not support deposition of eGFP-H2B onto amplifying EBV DNA (C) although they were expressed (D).

Figure S1

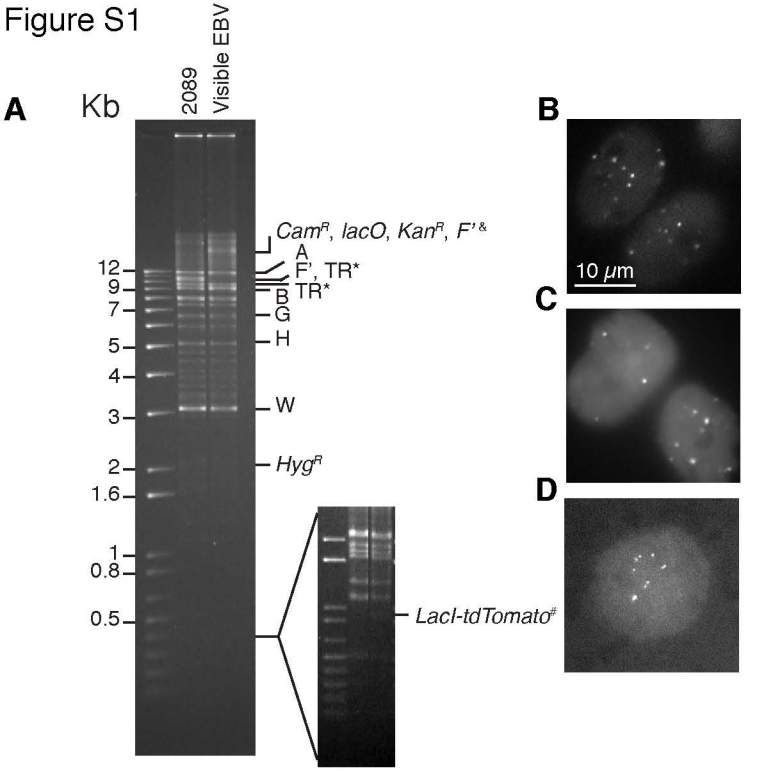

&, 26.5-kb of DNA fragment of *lacO-Kan*^{R}*-F'* Bacmid cassette
#, 0.9-kb of DNA fragment of *LacI-tdTomato-F'* Bacmid cassette gene
*, Variable terminal repeats (TR)

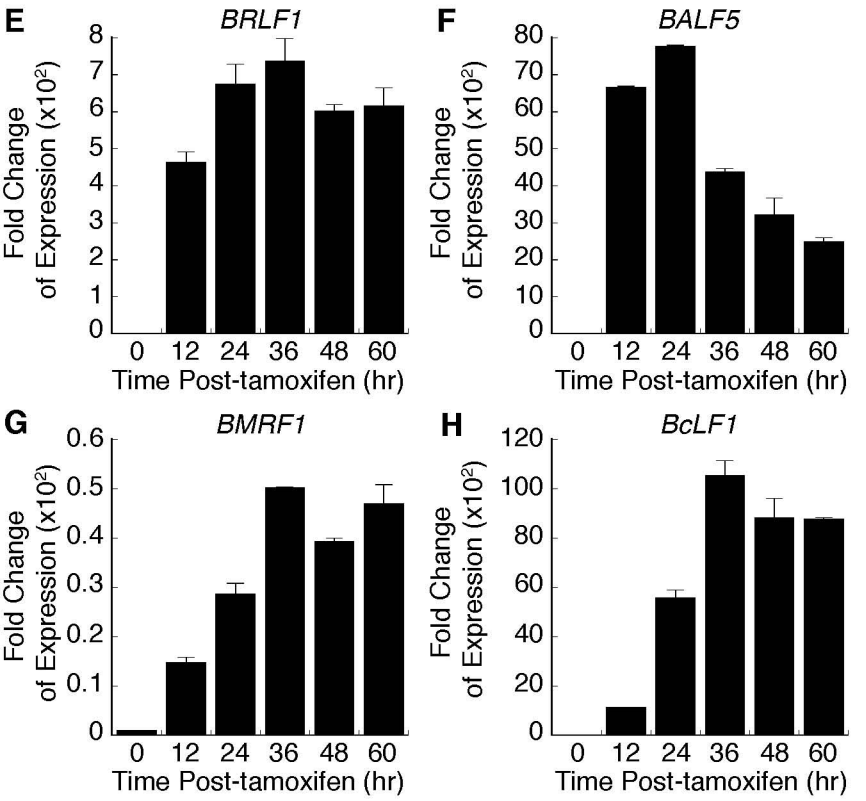

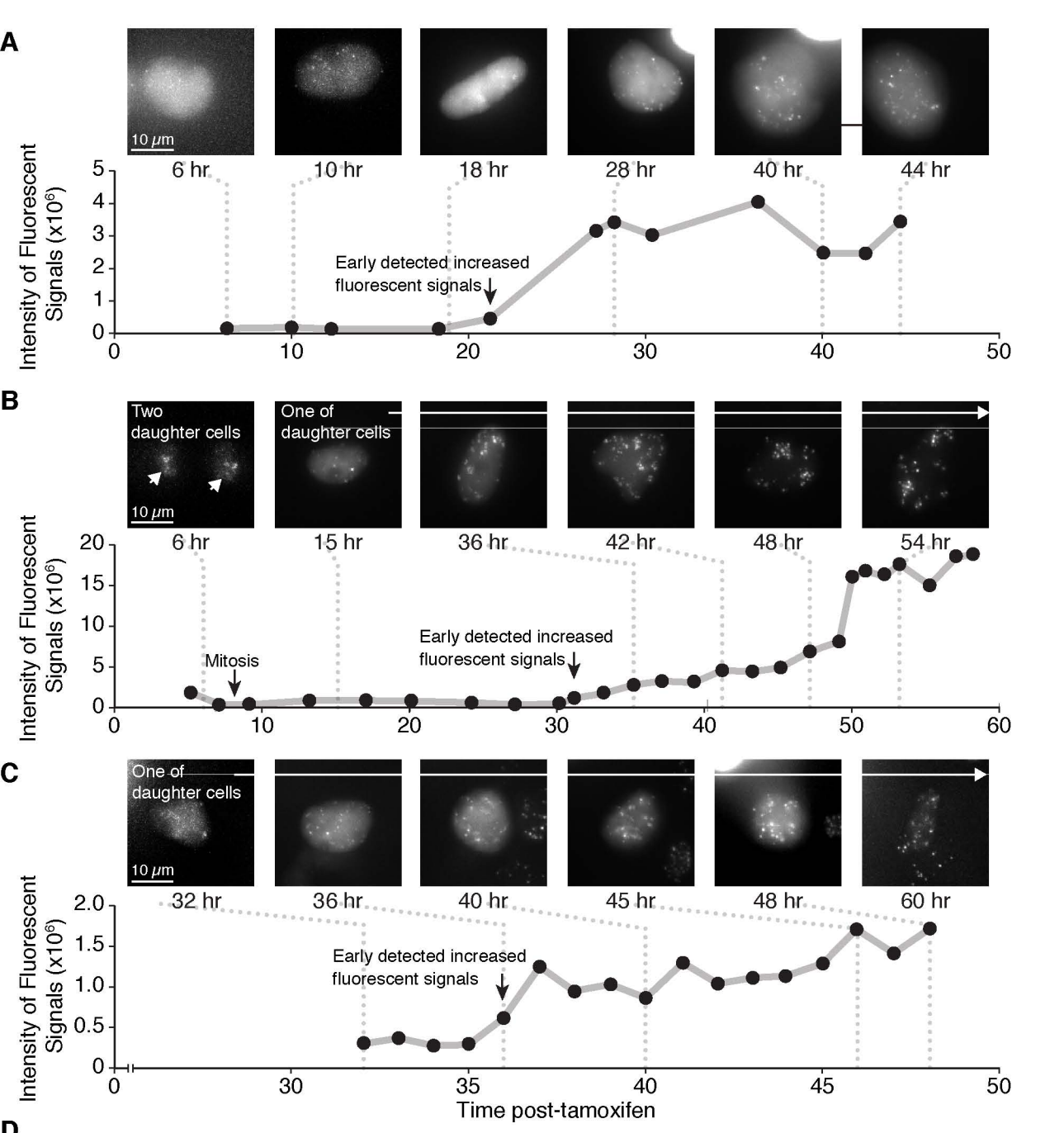
A
10 μm
6 hr
10 hr
18 hr
28 hr
40 hr
44 hr
Intensity of Fluorescent Signals (x10⁶)
Early detected increased fluorescent signals
B
Two daughter cells
One of daughter cells
10 μm
6 hr
15 hr
36 hr
42 hr
48 hr
54 hr
Mitosis
Early detected increased fluorescent signals
C
One of daughter cells
10 μm
32 hr
36 hr
40 hr
45 hr
48 hr
60 hr
Early detected increased fluorescent signals
Time post-tamoxifen

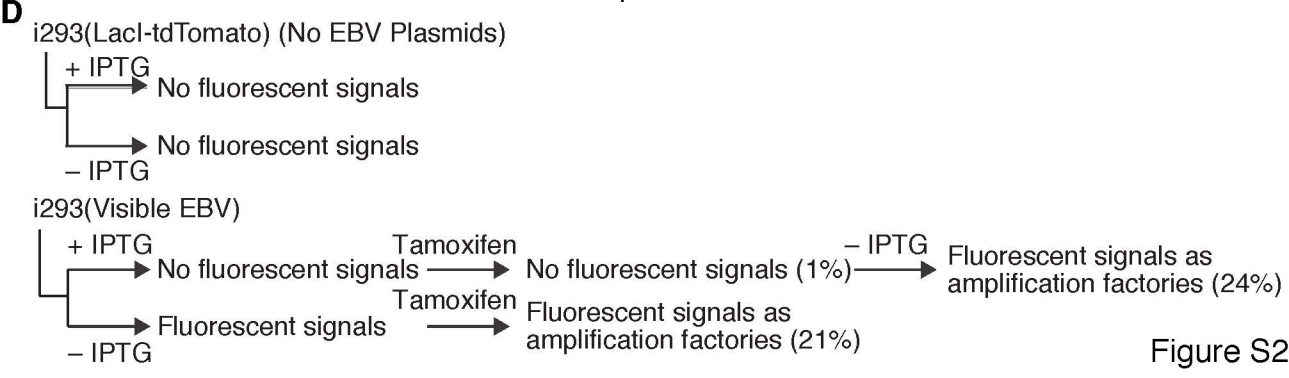
D
i293(LacI-tdTomato) (No EBV Plasmids)
+ IPTG
No fluorescent signals
No fluorescent signals
– IPTG
i293(Visible EBV)
+ IPTG
No fluorescent signals
Tamoxifen
No fluorescent signals (1%)
– IPTG
Fluorescent signals as amplification factories (24%)
Fluorescent signals
Tamoxifen
Fluorescent signals as amplification factories (21%)
– IPTG

Figure S2

Figure S3

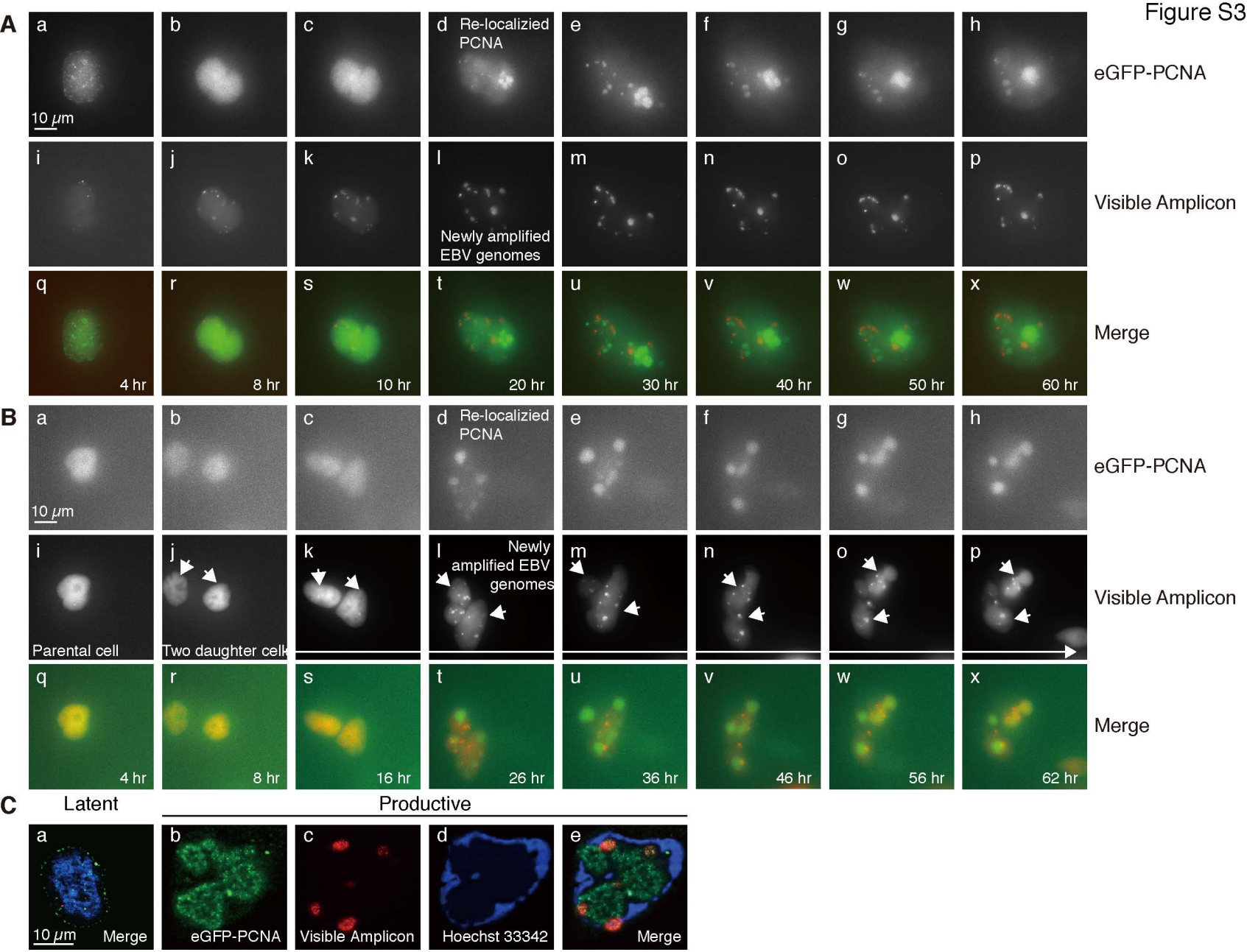
A
a
b
c
d Re-localizied PCNA
e
f
g
h
eGFP-PCNA
10 μm
i
j
k
l
Newly amplified EBV genomes
m
n
o
p
Visible Amplicon
q
r
s
t
u
v
w
x
Merge
4 hr
8 hr
10 hr
20 hr
30 hr
40 hr
50 hr
60 hr
B
a
b
c
d Re-localizied PCNA
e
f
g
h
eGFP-PCNA
10 μm
i
j
k
l Newly amplified EBV genomes
m
n
o
p
Visible Amplicon
Parental cell
Two daughter cells
q
r
s
t
u
v
w
x
Merge
4 hr
8 hr
16 hr
26 hr
36 hr
46 hr
56 hr
62 hr
C
Latent
Productive
a
b
c
d
e
10 μm
Merge
eGFP-PCNA
Visible Amplicon
Hoechst 33342
Merge

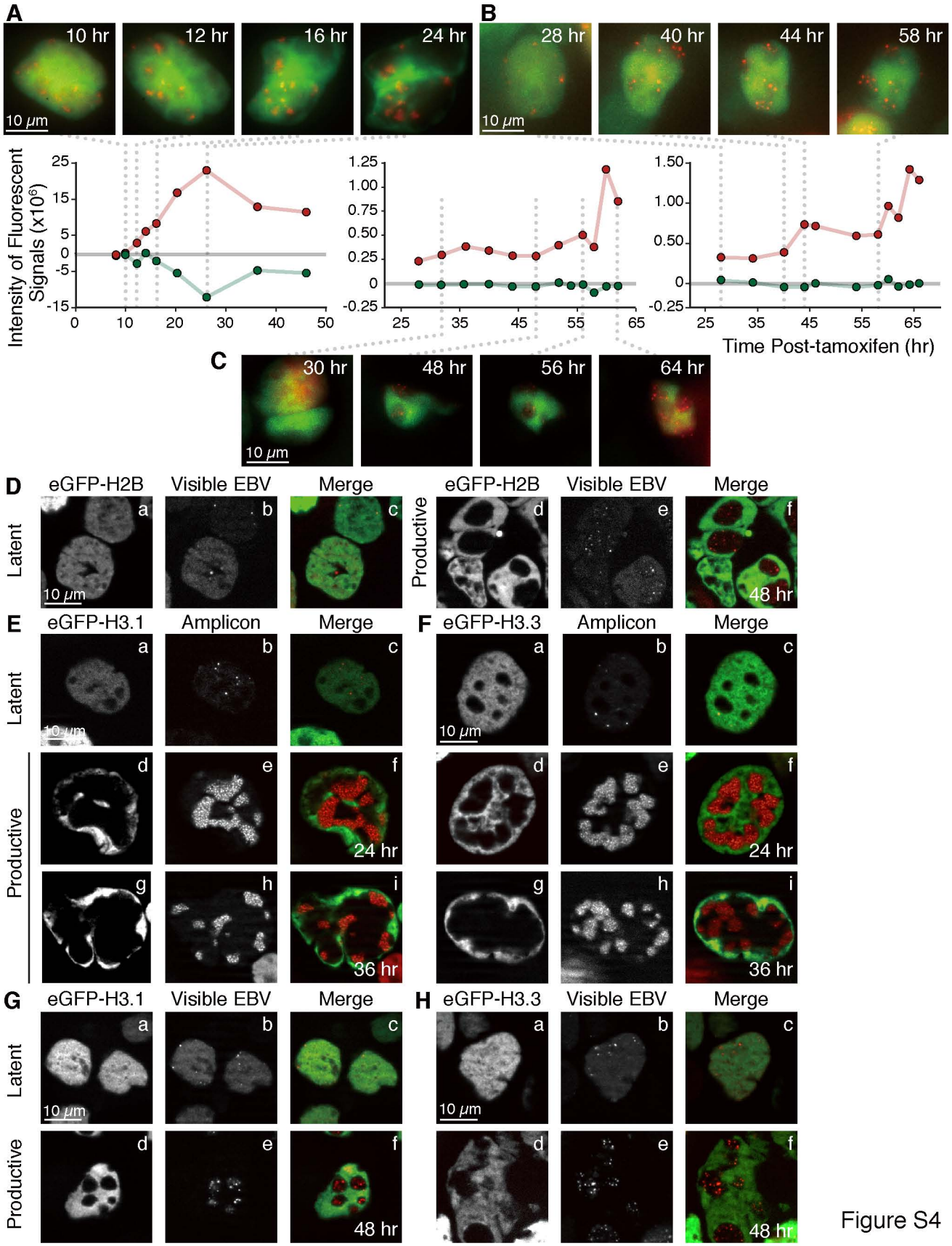
A
10 hr
12 hr
16 hr
24 hr
10 μm
B
28 hr
40 hr
44 hr
58 hr
10 μm
Intensity of Fluorescent Signals (x10⁶)
Time Post-tamoxifen (hr)
C
30 hr
48 hr
56 hr
64 hr
10 μm
D
eGFP-H2B
Visible EBV
Merge
Latent
Productive
48 hr
E
eGFP-H3.1
Amplicon
Merge
Latent
Productive
24 hr
36 hr
F
eGFP-H3.3
Amplicon
Merge
24 hr
36 hr
G
eGFP-H3.1
Visible EBV
Merge
Latent
Productive
48 hr
H
eGFP-H3.3
Visible EBV
Merge
48 hr

Figure S4

Figure S5

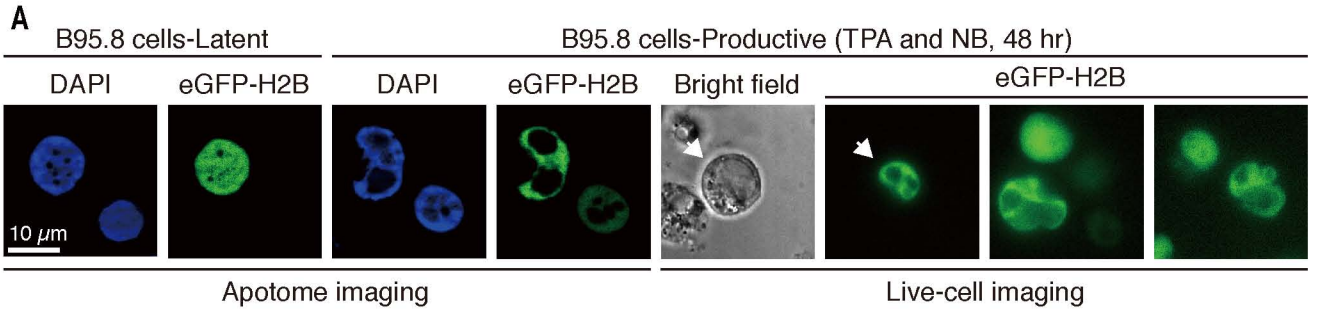
A
B95.8 cells-Latent
B95.8 cells-Productive (TPA and NB, 48 hr)
DAPI
eGFP-H2B
DAPI
eGFP-H2B
Bright field
eGFP-H2B
10 μm
Apotome imaging
Live-cell imaging

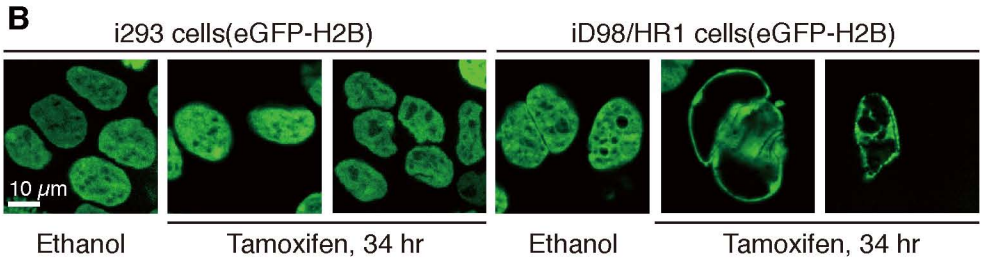
B
i293 cells(eGFP-H2B)
iD98/HR1 cells(eGFP-H2B)
10 μm
Ethanol
Tamoxifen, 34 hr
Ethanol
Tamoxifen, 34 hr

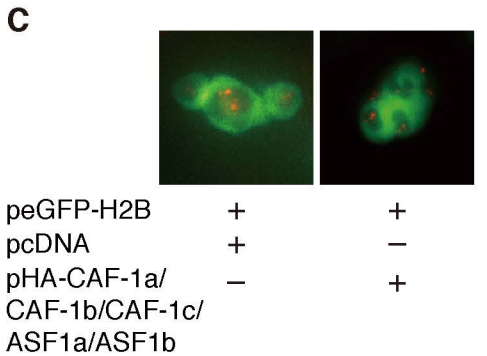
C
peGFP-H2B + +
pcDNA + –
pHA-CAF-1a/ CAF-1b/CAF-1c/ ASF1a/ASF1b – +

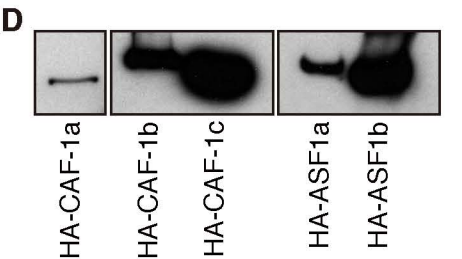
D
HA-CAF-1a
HA-CAF-1b
HA-CAF-1c
HA-ASF1a
HA-ASF1b

Supplemental Table S1, related to Experimental Procedures

Table S1: Primer and probe sequences used in this study.

Gene	Primer and Probe	Sequence
CHAF1A	Probe	6-FAM-TGAGGACGAAGGTGTGACAGAGGA-TAM
(CAF-1a)	Forward Primer	5' GAGGATGAAGATGAGGACGATG 3'
	Reverse Primer	5' TCCTTGGCCTTCAGTTTCTG 3'
CHAF1B	Probe	6-FAM-CTTCAGCCCCTATTCCAGACAGCAT-TAM
(CAF-1b)	Forward Primer	5' CGTGTGGCTTTCAATGTTTCG 3'
	Reverse Primer	5'TGAGAAGCAAAGATCCGTCG 3'
ASF1A	Probe	6-FAM-ACCAGCCCCAGTTCCCATTGTTT-TAM
	Forward Primer	5' CTGGACTTTATTGTGCCGC 3'
	Reverse Primer	5' CGGGTTGTAGAAAGGAGAAGG 3'
ASF1B	Probe	6-FAM-AAATGATCTTCCACTCCAGGTCGTCC-TAM
	Forward Primer	5' CCTTTCCACAGCCCCTTC 3'
	Reverse Primer	5' AAATTCCTCACTCTCAGCCG 3'
PCNA	Probe	6-FAM-CGGCTGAGACTTGCGTAAGGGAA-TAM
	Forward Primer	5' CTAGCCTGACAAATGCTTGC 3'
	Reverse Primer	5' AGGAAAGTCTAGCTGGTTTCG 3'
BRLF1	Probe	6-FAM-AGACGGGCGAGAATGCCGGC-TAM
	Forward Primer	5' TTGGGCCATTCTCCGAAAC 3'
	Reverse Primer	5' TATAGGGCACGCGATGGAA 3'
BMRF1	Probe	6-FAM-TCATAGCACTTGGACAGGACGGC-TAM
	Forward Primer	5' CACTCAGACTCTCCGCTTTAAG 3'
	Reverse Primer	5' GGGCCTCCATAGTTTACAGAC 3'
BALF5	Probe	6-FAM-TGTACACGCACGAGAAATGCGCC-TAM
	Forward Primer	5' CGGAAGCCCTCTGGACTTC 3'
	Reverse Primer	5' CCCTGTTTATCCGATGGAATG 3'
BcLF1	Probe	6-FAM-TCTTGTTTACGATCCATGCCTCCACC-TAM
	Forward Primer	5' GTGACAGAGAACCTTGAGAGC 3'
	Reverse Primer	5' CAATCCCAAGTACACGACCTC 3'
LacI	Probe	6-FAM-TGACCCAATGCGACCAGATGCT-TAM
	Forward Primer	5' GACCAGACACCCATCAACAG 3'
	Reverse Primer	5' CGCCGAGACAGAACTTAATGG 3'
GAPDH	Probe	6-FAM-TTCCTGGTATGACAACGAATTTGGCTACAGC-TAM
	Forward Primer	5' TCAACGACCACTTTGTCAAGCT 3'
	Reverse Primer	5' CCATGAGGTCCACCACCCT 3'

Supplemental Experimental Procedures

Cell lines and culture

HEK293, 293T, and EBV-positive D98/HR1 cells were grown in DMEM containing 10% fetal bovine serum. Primary B cells, B95.8 and EBV-negative Daudi cells were grown in RPMI1640 containing 10% fetal bovine serum. All cells were maintained in a humidified 5% CO_2 incubator at 37ºC.

Plasmids

BZLF1 cDNA was amplified by PCR with primer (5' CGCGGATCCGAGAAATTTAAGAGATCCTCGTGTAAAACATCTGG 3' and 5'CCGGAATTCATGATGGACCCAAACTCGACTTCTGAAG 3') using pSG5-Z provided kindly by Dr. Shannon Kenney as a template and digested with *Eco*RI and *Bam*HI; a DNA fragment encoding the estrogen receptor-binding domain (ERTAM) was digested with *Bam*HI and *Mlu*I from p3560. The *BZLF1* cDNA and DNA fragment with the *ERTAM* gene were then inserted into the *Mfe*I-*Mlu*I site of a retroviral vector, p3048, to yield p3872. A Klenow-filled *Bam*HI/*Xho*I fragment of p3621 encoding eGFP-Histone H2B fusion was inserted into the *Hpa*I-*Xho*I site of p3048 to yield p3803. *HIST1H3C* and *H3FB* were amplified by PCR using pOZ-e-H3.1 and pOZ-e-H3.3 (Tagami et al., 2004) as templates, respectively, with the primer pair (5' TCAGATCTATGGCTCGTACGAAG 3'; 5' TCGGATCCTGCCCTTTCCCCACG 3') and (5' TCAGATCTATGGCCCGAACCAAG 3'; 5' TCGGATCCAGCTCTCTCTCCCCG

3'), respectively, digested with *Bgl*II and *Bam*HI, and inserted into the *Bgl*II-*Bam*HI site of pEGFP-C1 (Clontech) to yield plasmids expressing eGFP-H3.1 and eGFP-H3.3 fusions, respectively. DNA fragments encoding the eGFP-H3.1 or eGFP-H3.3 fusions were amplified, digested with *Eco*RI and *Xho*I, and then inserted into the *Mfe*I-*Xho*I site of p3048 for ectopic expression. A klenow-filled *Age*I-*Xba*I fragment of pENeGFP-PCNAL2mut encoding an eGFP-PCNA fusion (Leonhardt et al., 2000) was inserted into the *Hap*I site of p3048 for ectopic expression. *CAF-1B* (*CAF-1 p60*) was amplified by PCR with the primer pair (5' ATGCA CCCGGGTTCCCCTTCGAGACTCAGGAGGATG 3'; 5' ATGCACTCGAG AAGGGTCCAGACTTTCCGTGCCTC 3'), digested with *Sma*I-*Xho*I, and inserted into the *Eco*RV-*Xho*I site of pcDNA-HA2 to yield a plasmid expressing a HA-tagged CAF-1 p60 fusion. *CAF-1C* (*CAF-1 p48*) was amplified by PCR with the primer pair (5' CCGGAATTCATGGCCGACAAGGAAGCAGCCT 3'; 5' ATGCACTCGAGAGGACCCTTGTCCTTCTGGATCCACG 3'), digested with *EcoR*I-*Xho*I, and inserted into the *Eco*RI-*Xho*I site of pcDNA-HA2 to yield a plasmid expressing a HA-tagged CAF-1 p48 fusion. The human cdt1 (residues 30-120) was digested from pTRE-cellcycle (Clontech) with *Eco*RV and *Bgl*II and inserted into the *Eco*RI(Klenow)-*Bam*HI site of pEGFP-C1. A Klenow-filled *Nhe*I-*Hpa*I fragment of pEGFP-hcdt1 encoding the eGFP-cdt1(30-120) fusions was then inserted into the *Hpa*I site of p3048 for ectopic expression. pMH009, pPK71, and pPK70 expressing Flag-HA-tagged CAF-1a, CAF-1b, and CAF-1c, respectively, were provided kindly by Dr. Bruce Stillman. pcDNA-HA-ASF1a and pHA-ASF1b expressing HA-tagged ASF1a and HA-tagged ASF1b, respectively,

were provided kindly by Dr. Peter Adams. A Klenow-filled *Xba*I/*Bgl*II fragment of p4001 encoding the LacI-tdTomato fluorescent fusion along with NLS signal was inserted into the *Bam*HI-*Sma*I site of p1958 to yield p4002 in which LacI-tdTomato fluorescent protein was transcribed from the SV40 early promoter. The DNA fragment containing the SV40 early promoter and *LacI-tdTomato-NLS* was then amplified by using primers (5' GCGCCCGGGGACTTCTGAGGCGGAAAGAACCAGCTGTGG 3' and 5 CGGGAGCTCTGAGCGAGGAAGCGGAAGAGTCTAGAGTCG 3'), digested with *Sma*I and *Sac*I, and inserted behind the Kan^R and 250 copies of *lacO* sites of p3686 at the *Stu*I-*Sac*I site to generate p4003.

Generation of Visible Amplicon

The DNA fragment of *lacO-*KAN^R*-SV40 promoter-LacI-tdTomatoNLS* digested with *Pvu*I from p4003 was then inserted into the *Pvu*I site of p3944, which is a derivative of plasmid 588 (Bloss and Sugden, 1994) with $G418^R$ replacing Hyg^R, to generate a Visible Amplicon (or p4012).

Generation of Visible EBV

The DNA fragment of *lacO-*KAN^R*-SV40 promoter-LacI-tdTomatoNLS* digested with *Sma*I and *Sac*I from p4003 was then inserted into the *Spe*I-*Sac*I site of a shuttle vector, p3194, which contains the sequences homologous to the bacmid cassette on the EBV recombinant 2089, to yield p4004. p4004 linearized by *Pac*I and *Not*I was electroporated into *E. coli* DH10B(pKD46, EBV Bacmid 2089) to

generate Visible EBV (or p4016) via Red-mediated recombination.

The visible EBV bacmids isolated from single outgrowing bacterial colonies were digested with the restriction enzyme, *Nco*I, and analyzed by Southern Blotting to ensure that they contained approximately 250 copies of *lacO* sites (Data not shown). Furthermore, the *Bam*HI restriction patterns of both parental EBV recombinant 2089 and visible EBV were analyzed to ensure their integrity (fidelity). As expected, all the *Bam*HI-fragments in both EBV recombinants were identical except for DNA fragments with *lacO, Kan^R, LacI-tdTomato,* F-replicon cassette, and the variable number of terminal repeats sequence (see Figure S1A) (Delecluse et al., 1998; Kintner and Sugden, 1981).

Quantification of encapsidated viral genomes

The amount of encapsidated viral DNA was determined according to a method described elsewhere (Chiu et al., 2012). The culture medium from iD98/HR1 or i293 cells was collected at 3 days or 5 days, respectively, after treatment with 200 nM of tamoxifen followed by centrifugation to remove cell debris, treatment with DNase to eliminate non-ecapsidated DNAs, and subsequent proteolytic digestion to remove the capsid proteins. The encapsidated viral DNA was then extracted by phenol-chloroform, precipitated, and quantified by qPCR with primers and probe specific to BALF5 shown in Table S1.

Retroviral transduction

Retroviral vectors were generated in 293T cells as previously described with

modifications (Vereide et al., 2013). Briefly, retrovirus was generated by co-transfecting 293T in a 70% confluent 10-cm dish with 3 µg of a plasmid encoding Gag-Pol, 1 µg of a plasmid encoding the vesicular stomatitis virus G protein, 1 µg of a plasmid encoding a derivative of NF-κB, and 10 µg of a plasmid carrying the retroviral backbone containing genes encoding BZLF1 fused to estrogen receptor ligand binding-domain (Z-ER) and resistance to puromycin using lipofectamine 2000. The viruses were collected from culture medium after 24 and 48 hr after transfection followed by sedimentation in rotor 50Ti at 25,000x rpm for 2 hr. D98/HR1 and 293 cells were then incubated with concentrated viral stocks at 4ºC for one hour followed by 37ºC for 48 hr for retrovirus infection.

Isolation and infection of human primary B lymphocytes.

Human peripheral blood mononuclear cells (PBMC) were separated from whole blood by Ficoll□Hypaque gradient centrifugation. B-cells were purified from PBMCs using the B-cell isolation kit II (Miltenyi Biotec, Gladbach, Germany) and MACS separators (Miltenyi Biotec). For virus infection, primary B cells were incubated and rocked with viral stocks at 4ºC for one hour followed by replacement with fresh medium and incubation at 37ºC for 48 hrs. Virus stocks were titered on EBV-negative Daudi cells.

Computer-Assisted Plasmid Summation (CAPS)

CAPS combines annulus-background subtraction photometry from astronomy with microscopic z-planes. CAPS consists of two libraries of code. The first is a

GPU-accelerated library to display time-series of z-planes and to perform simple photometry. 16-bit images are converted to display linearly, exponentially, or a combination of the two with the display range automatically set to the minimum and maximum of an image. Multiple z-planes are displayed simultaneously to aid plasmid identification. The second library tracks and saves plasmids, displays changes over time, fits plasmid profiles, and allows for cell differentiation. Plasmid positions from one image can be applied to others to compare different fluorescent markings or integration times. These libraries are available for download and are designed to be extended to include other image formats. We chose to implement CAPS in pure javascript rather than as a plugin for ImageJ so that we could collect information from time-series, share data across multiple computers, display different z-planes concurrently, and control the 16-bit to 8-bit translation function.

Subtraction of the background intensity behind a plasmid is essential (Figure 2A-B). The flux from a fluorescently-labeled plasmid may make up only 1% of the total flux of the pixels it covers due to a combination of autofluorescence and camera noise. Point-sources of light, smaller than one-tenth of the pixel resolution, ideally form Airy discs which are well-represented by a Gaussian distribution. Single plasmids approximate point-sources (Figure 2). Using a best-fit Gaussian distribution, it is easy to determine the radius that contains at least 95% of the flux. This radius, from the normal distribution, is 1.96 sigma. By determining the minimum area covered by a plasmid, one can measure the average background behind the plasmid from an annulus of one

pixel surrounding the plasmid. Measuring the local background is essential; the nucleus often varies by more than the intensity of a single plasmid. This method of measurement of intensity is reproducible. Measurements of intensities of signals of Visible EBV were made after deconvolving the images with the Zeiss software, Axiovision, using a theoretical point spread functions.

Immunoblotting

Immunoblotting was performed as described (Vereide et al., 2013); the blots were probed with Anti-CAF-1a (#5480, Cell signaling), anti-ASF1a (#2990, Cell signaling), anti- Histone H2B (ab1790, Abcam), anti-Histone H3 (FL-136, sc-10809, Santa Cruz), anti-HIRA (ab20655, Abcam), anti-NAP1L1 (ab21630, Abcam), anti-PCNA (clone EPR3821, LS-C105652, Lifespan biosciences), anti-BMRF1 (Clone G3-E31, VP-E608, Vector Laboratory), anti-alpha-tubulin (clone DM1A, T6199, Sigma), anti-Daxx (D7810, Sigma), anti-HA (Clone HA-7, H9658, sigma) followed by Horseradish Peroxidase□labeled secondary antibodies (KPL) and detected with supersignal west pico chemiluminescent substrate (Thermo). The signals were quantified using Image J.

RNA isolation and reverse transcription

Total RNA was isolated from $5x10^6$ cells using Qiagen RNeasy mini columns following the manufacture's protocol (Qiagen) and treated with TURBO DNase (Invitrogen) to eliminate the contamination of DNA followed by cDNA preparation with SuperScript VILO cDNA synthesis kit following manufacture's protocol

(Invitrogen).

Real-time PCR (qPCR) analysis

Measurements were conducted as described elsewhere (Vereide and Sugden, 2011). Probes were labeled with 5'□FAMRA and 3'□TAMRA (IDT, Integrated DNA Technologies, Coralville, IA). Primer and probe sequences are listed in Table S1.

Supplemental References

Bloss, T.A., and Sugden, B. (1994). Optimal lengths for DNAs encapsidated by Epstein-Barr Virus. J Virol *68*, 8217-8222.

Chiu, Y.F., Sugden, B., Chang, P.J., Chen, L.W., Lin, Y.J., Lan, Y.C., Lai, C.H., Liou, J.Y., Liu, S.T., and Hung, C.H. (2012). Characterization and intracellular trafficking of Epstein-Barr Virus BBLF1, a protein involved in virion maturation. J Virol *86*, 9647-9655.

Delecluse, H.J., Hilsendegen, T., Pich, D., Zeidler, R., and Hammerschmidt, W. (1998). Propagation and recovery of intact, infectious Epstein-Barr Virus from prokaryotic to human cells. Proc Natl Acad Sci U S A *95*, 8245-8250.

Glaser, R., and Rapp, F. (1972). Rescue of Epstein-Barr Virus from somatic cell hybrids of Burkitt lymphoblastoid cells. J Virol *10*, 288-296.

Kintner, C., and Sugden, B. (1981). Conservation and progressive methylation of Epstein-Barr Viral DNA sequences in transformed cells. J Virol *38*, 305-316.

Leonhardt, H., Rahn, H.P., Weinzierl, P., Sporbert, A., Cremer, T., Zink, D., and Cardoso, M.C. (2000). Dynamics of DNA replication factories in living cells. J Cell Biol *149*, 271-280.

Tagami, H., Ray-Gallet, D., Almouzni, G., and Nakatani, Y. (2004). Histone H3.1 and H3.3 complexes mediate nucleosome assembly pathways dependent or independent of DNA synthesis. Cell *116*, 51-61.

Vereide, D.T., Seto, E., Chiu, Y.F., Hayes, M., Tagawa, T., Grundhoff, A., Hammerschmidt, W., and Sugden, B. (2013). Epstein-Barr Virus maintains lymphomas via its miRNAs. Oncogene.

Vereide, D.T., and Sugden, B. (2011). Lymphomas differ in their dependence on Epstein-Barr Virus. Blood *117*, 1977-1985.